Temperature Tuning of Nonlinear Exciton Processes in Self-Assembled Oligophenyl Nanofibers under Laser Action**

By *Francesco Quochi,* Michele Saba, Fabrizio Cordella, Agnieszka Gocalinska, Riccardo Corpino, Marco Marceddu, Alberto Anedda, Andrei Andreev, Helmut Sitter, Niyazi Serdar Sariciftci, Andrea Mura,* and *Giovanni Bongiovanni*

Organic semiconductors have long been investigated for their potential of enhancing laser technology owing to their large conversion efficiency, gain cross-section, and bandwidth.[1] Oligophenylene-based π-conjugated materials, having high carrier mobilities (up to $14\,cm^2\,V^{-1}\,s^{-1}$[2]) and emission yields (ca. 30%[3]), represent an important class of organic semiconductors for which amplified spontaneous emission (ASE) and low-threshold lasing action have been achieved in single crystals and ordered thin films.[4,5] The last decade has also witnessed great advances in the growth of ordered oligophenylenes thin films with enhanced optoelectronic properties, for example, through surface dipole-assisted heteroepitaxy.[6–8] The resulting needle-shaped aggregates, usually referred to as nanofibers, feature charge-carrier mobilities that range from ca. 10^{-2} to ca. $10\,cm^2\,V^{-1}\,s^{-1}$, depending on fabrication technique,[2,9] self-guiding of optical emission for light amplification, and lasing under femtosecond excitation.[10,11] In particular *para*-sexiphenyl (*p*-6P) nanofibers have been highlighted as prototypical material system for self-assembled organic lasers, with large stimulated-emission cross-section

(ca. $2 \times 10^{-16}\,cm^2$), ultrawide (ca. 1 eV) gain bandwidth, long (ca. 1 ns) gain lifetime,[12] and potential for the development of high-sensitivity nonlinear optical nanosensors.[12–14]

Excellent gain properties measured under ultrafast femtosecond excitation do not, however, necessarily translate into low lasing thresholds. When organic crystals are excited by slowly-varying light sources, additional intrinsic losses appear. In particular, bimolecular recombination is a very efficient nonradiative, density-dependent decay pathway of singlet excitons in crystalline oligophenyl films.[15–17] Singlet–singlet annihilation shortens the gain lifetime and thus contrasts gain build-up under nanosecond pumping conditions; in addition, it promotes the population of gain-quenching intermolecular (''charge-transfer'') excitons.[12,18] As a consequence, nonlinear losses stand as a big obstacle to the further development of organic-crystal lasers that operate in more convenient timescale regimes and with lower thresholds. The potential of high-mobility organic crystals and ordered thin films as viable laser media rests on quantitative understanding and control of exciton nonlinearities, as highlighted by a very recent report of single-crystal field-effect transistors with constant quantum efficiency for current densities up to hundreds of amperes per square centimeter, close to the expected threshold of amplified spontaneous emission.[19]

In this Communication, we present an experimental study on laser action in self-assembled *p*-6P nanofiber films, where random optical feedback for light propagating along the fibers is provided by tiny fiber breaks.[20] Different dynamical regimes were accessed using femto- and nanosecond-pulsed excitation. Sample temperature was used as a knob to tune the rate of singlet–singlet annihilation over one order of magnitude, making it possible to achieve laser action in the linear (monomolecular) recombination regime, and thus to fully exploit the potential of crystalline *p*-6P as a gain medium even with slowly varying optical excitation.

Temperature dependence of the excited-state recombination dynamics in *p*-6P nanofibers under ultrafast photoexcitation was studied in a film exhibiting an average fiber height (h) of 300 nm, fiber filling factor (η; i.e., the fraction of substrate surface covered with nanofibers) close to 100%, and large ASE threshold fluence values (ca. 100–200 $\mu J\,cm^{-2}$), therefore suitable to retrieve the intrinsic excited-state dynamics not perturbed by stimulated emission. High thresholds are possibly

[*] Dr. F. Quochi, Dr. M. Saba, Dr. F. Cordella, A. Gocalinska, Dr. R. Corpino, Dr. M. Marceddu, Prof. A. Anedda, Prof. A. Mura, Prof. G. Bongiovanni
Dipartimento di Fisica
Università degli Studi di Cagliari
09042 Monserrato (Italy)
E-mail: francesco.quochi@dsf.unica.it
Dr. A. Andreev
Institute of Physics
University of Leoben
8700 Leoben (Austria)
Prof. H. Sitter
Institute of Semiconductor and Solid State Physics
Johannes Kepler University Linz
4040 Linz (Austria)
Prof. N. S. Sariciftci
Linz Institute for Organic Solar Cells (LIOS) Physical Chemistry
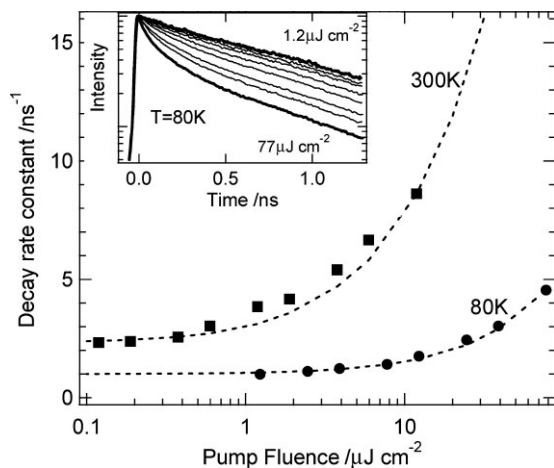Johannes Kepler University Linz
4040 Linz (Austria)

Figure 1. Characteristic inverse decay times of the optical emission intensity of p-6P nanofibers excited by 150 fs long pulses at 360 nm wavelength. Squares: room-temperature data; circles: data at $T = 80$ K. Dashed lines: Calculations with: $k_0 = 1 \times 10^9$ (2.3×10^9) s^{-1}, $\kappa_{SS} = 3 \times 10^{-9}$ (4×10^{-8}) cm^3 s^{-1} for $T = 80$ (300) K. Inset: Decay traces at 80 K integrated over the 0–1 vibronic band of p-6P for excitation fluence of 1.2, 2.5, 3.9, 7.8, 12, 25, 39, and 77 μJ cm^{-2} per pulse.

caused by efficient out-of-plane light scattering, detrimental to waveguiding and optical feedback.[21] Results are summarized in Figure 1, which displays the fluorescence decay rate constant as a function of excitation fluence. A series of fluorescence decay traces taken at $T = 80$ K is shown in the inset of Figure 1, clearly demonstrating that at high pump fluences the singlet recombination dynamics is dominated by nonradiative, density-dependent processes that are ascribed to singlet–singlet (bimolecular) annihilation.[12,15]

Bimolecular recombination however turns out to strongly depend on lattice temperature. Upon fitting the $1/e$ decay times with the results of numerical simulations of the singlet recombination dynamics, we estimate that the singlet bimolecular coefficient (κ_{SS}) lowers from 4×10^{-8} to 3×10^{-9} cm^3 s^{-1} for a decrease in temperature from 300 to 80 K.[22] We note that also the linear recombination rate constant (k_0) exhibits a temperature dependence, lowering from 2.3×10^9 to 1×10^9 s^{-1} for the same temperature drop. At $T = 80$ K, bimolecular processes kick in for pump fluences around a few microjoules per square centimeter, while at room temperature the linear recombination regime holds only up to excitation fluences on the order of 0.1 μJ cm^{-2}. The physical origin of temperature dependence of the bimolecular coefficient can be traced back to energetic disorder in these crystalline p-6P nanostructured films,[23] which is thought to provide thermal activation for exciton migration and hence exciton-exciton interactions.[24]

Direct demonstration of lasing in the regime of linear, that is, monomolecular, recombination of singlet excitons was provided in a film with $h \sim 100$ nm and $\eta \sim 50\%$, a sample characterized by efficient random feedback and therefore low lasing threshold. The results of femtosecond-pulsed excitation on a low-loss region of the nanofiber film are shown in Figure 2, where the low-temperature ($T = 80$ K) optical emission intensity resolved both in time and wavelength is plotted on
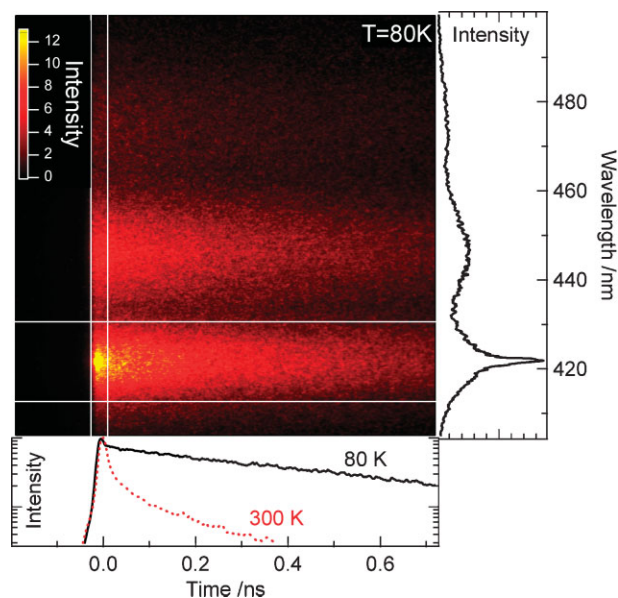

Figure 2. False-color streak image of the temporally and spectrally resolved emission intensity of p-6P nanofibers at $T = 80$ K; excitation pulses are 150 fs long and centered in wavelength at 360 nm; excitation fluence: 7 μJ cm^{-2} per pulse. Vertical (horizontal) white lines delimit the area for temporal (spectral) integration. Right panel: emission spectrum, integrated in the first 30 ps after excitation pulse arrival, showing prompt laser action. Bottom panel: Emission decay traces integrated over the 0–1 vibronic band of p-6P. The solid (dashed) line is the time profile at $T = 80$ (300) K.

a false-color scale. The excitation fluence (ca. 7 μJ cm^{-2}) was about a factor of two above the lasing threshold fluence (ca. 4 μJ cm^{-2}). In the right-hand side panel the emission spectrum integrated over the first 30 ps after excitation is reported, with the typical vibronic progression of p-6P fluorescence and laser emission superimposed onto the 0–1 vibronic band. The time profile of the emission (bottom panel) demonstrates that the prompt laser emission, which was temporally unresolved by the detection system, left the system with a population of singlets undergoing monomolecular recombination.

Raising the temperature from 80 to 300 K produced a shortening of fluorescence lifetime owing to bimolecular recombination, as visible in the bottom panel of Figure 2, but did not significantly alter the lasing threshold fluence under femtosecond excitation. Owing to the ultrafast injection of singlet excitons in the active medium, lasing threshold with femtosecond-pulsed excitation is indeed expected to be determined predominantly by feedback losses and other linear optical losses such as ground-state absorption, while only weakly affected by excited-state lifetime shortening and photoinduced absorption of secondary excitations.[25] In fact, photoinduced absorption of primary singlet and triplet excitons overlaps with gain only at low energies,[12,26] while near-gap photoinduced absorption is fully effective only upon activation of charge-transfer excitons (tens to hundreds of picoseconds after photoexcitation).[12,18]

To translate monomolecular lasing into a significant milestone, one has however to demonstrate how lasing performance

scales with increasing duration of excitation pulses, as useful devices would require pulses not shorter than a few nanoseconds, favoring accumulation of long-lived charge-transfer excitons. Nanofiber lasing in the low-threshold sample was therefore investigated with nanosecond excitation (see the inset in Fig. 3 for laser pulse and gate temporal profiles). To ensure a meaningful comparison of femto- and nanosecond measurements, care was taken so as to always excite the same sample area, as illuminating fibers over different areas could modify the amount of optical feedback. Figure 3 shows time-integrated emission spectra measured for various excitation intensities at 80 K. The lasing threshold occurs for pump fluences of ca. 16 kW cm^{-2}, just two times higher than what one would expect in the absence of nonlinear losses with a monomolecular decay rate $k_0 \sim 1.5 \times 10^9$ s^{-1}, as extracted from linear measurements in the low-threshold, 100 nm thick sample. The low threshold is a strong indication that at 80 K the accumulation of charge-transfer excitons over the 4 ns duration of excitation pulses does not significantly change the lifetime and cross-section of gain. A dramatic display of the importance of nonlinear losses comes from the ca. 50-fold increase in nanosecond threshold pump intensity, from 16 to 800 kW cm^{-2}, recorded when the temperature was raised from 80 to 300 K. This finding has to be contrasted with the almost equal femtosecond lasing thresholds at 80 and 300 K. Several film regions made of nanofibers with higher threshold fluences (under femtosecond pumping) did not even show any lasing action at room temperature under nanosecond-pulse excitation.

Numerical simulations of the system dynamics highlight the role played by secondary charge-transfer excitons for nanosecond-pulsed excitation at room temperature. Activation of a population density (N_{CT}) of charge-transfer excitons is introduced on the basis of the above-mentioned reaction scheme,[18] with a total rate of formation equal to $\kappa_{SS} N_S^2 / 4$
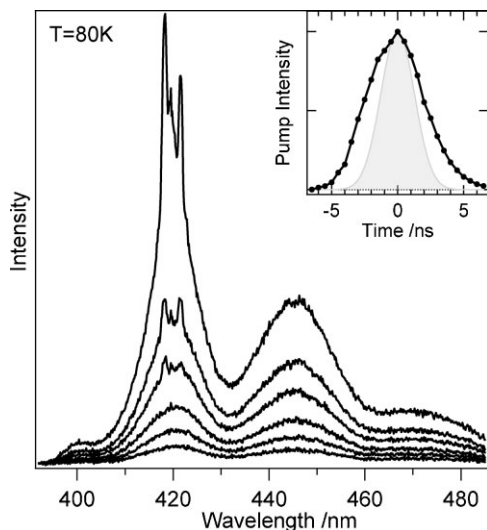
(where N_S is the singlet exciton density and κ_{SS} the singlet–singlet annihilation coefficient). The photon density (N_P) is described in single-mode approximation by:

$$dN_P/dt = +\varepsilon \, k_R \, N_S + \sigma_{SE} v \, N_P N_S - \sigma_{PA} v \, N_P N_{CT}$$
$$- k_L \, N_P \tag{1}$$

where ε is the fraction of spontaneous emission captured into the lasing mode, k_R the radiative emission rate constant of singlet excitons, $\sigma_{SE(PA)}$ the stimulated emission (photoinduced absorption) cross-section of singlet (charge-transfer) excitons, v the speed of light in the medium, and k_L the linear optical loss constant of the lasing mode. Parameter values were: $\varepsilon = 10^{-4}$, $k_R = 0.7 \times 10^9$ s^{-1} ($k_R/k_0 \sim 0.3$), $\sigma_{SE} = 2 \times 10^{-16}$ cm^2, $\sigma_{PA} = 1 \times 10^{-17}$ cm^2 (the ratio σ_{PA}/σ_{SE} is consistent with previous differential transmission measurements[12]). The temperature-dependent values of the singlet exciton recombination constants (k_0, κ_{SS}) are extracted from measured data. Charge-transfer excitons are assumed to recombine into singlet excitons with a characteristic time of 1 ns. 4 ns long Gaussian-shaped pump pulses have 100% conversion efficiency into singlet excitons across a 100 nm thick film. The singlet-exciton generation rate is thus given by $G(t) = I(t)/(E_p d)$, with $I(t)$ being the pump intensity profile, E_p the pump photon energy, and d the film thickness.

Figure 4 shows the calculated lasing threshold intensity versus total linear loss coefficient $\alpha_L = k_L/v$ or, alternatively, threshold density [$N_{th}^{(L)} = \alpha_L/\sigma_{SE}$] for lasing action assuming
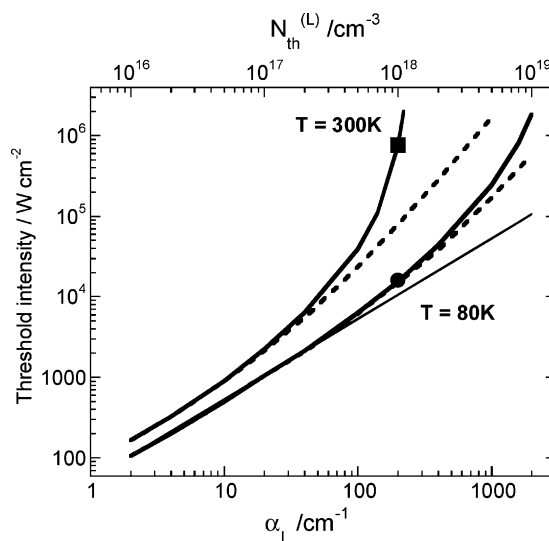

Figure 3. Emission spectra of *p*-6P nanofibers kept at $T = 80$ K and excited by 4 ns long pulses at 380 nm. Excitation intensities are 3.6, 7.2, 14, 18, 29, and 72 kW cm^{-2}. Inset: Temporal profiles of the pump intensity (dotted curve) and gate window (shaded curve).

Figure 4. Calculated lasing threshold intensity of a *p*-6P nanofiber film versus linear optical loss coefficient (α_L) and linear singlet threshold density [$N_{th}^{(L)}$]. Pulsed excitation with 4 ns long pulses is assumed. Continuous lines: bimolecular recombination and photoinduced absorption are both included in the calculations; Dashed lines: photoinduced absorption is turned off. The thin straight line highlights the lasing response of the same nanofiber film in the absence of bimolecular recombination (at $T = 80$ K). Solid symbols are the experimental data obtained with nanosecond-pulsed excitation.

only linear losses, which holds good for femtosecond-pulsed excitation. For small linear loss values, lasing threshold is reached in the regime of monomolecular recombination, thus threshold intensity increases linearly with loss coefficient. For high-enough values of α_L, this dependence turns superlinear owing to the increasingly important contribution of bimolecular recombination. This is summarized by the dashed lines, where photoinduced absorption of charge-transfer excitons is turned off (setting $\sigma_{PA} = 0$). Once photoinduced absorption is enabled (solid lines in Fig. 4), the combined effect of bimolecular recombination and nonlinear optical losses introduced by secondary excitations on the system performance becomes evident. At room temperature, the result is a dramatic increase of threshold intensity with increasing α_L within the loss range of interest for random lasing in our nanofibers. Calculations done with the singlet decay parameters corresponding to $T = 80$ K highlight that lattice cooling increases the range of optical losses compatible with monomolecular lasing. The experimental data of lasing threshold intensity under ns-pulsed pumping (full markers in Fig. 4) are consistent with this model picture assuming an average α_L value of 200 cm^{-1} in the investigated nanofibers. This corresponds to a singlet population at threshold of $N_{th}^{(L)} = 1 \times 10^{18}$ cm^{-3} or, equivalently, threshold femtosecond-pulsed fluence ~ 5.5 μJ cm^{-2}, in reasonable agreement with measured values. Further, these calculations elucidate why nanofibers with higher losses fail to reach nanosecond-pulsed lasing threshold at room temperature for pump intensities as high as ca. 5 MW cm^{-2}.

The results of the simulation provide us with a broad outlook beyond experimental results presented here, as they show that instead of resorting to cryogenic temperatures, the monomolecular lasing regime could be achieved at room temperature by acting on optical losses. The target for best performance is reduction of the internal and feedback losses to ca. 10 cm^{-1}, a value that seems attainable with established processing techniques for organic devices and that would limit the power density necessary to induce lasing to values below 1 kW cm^{-2}, low enough to enable indirect pumping with compact nanosecond lasers. Crystal doping, for example, by co-evaporation techniques, is envisaged as a viable strategy for effective material functionalization: efficient Förster energy transfer from the molecular crystal donor to chromophore acceptors emitting at lower photon energies would in fact allow for fast immobilization of excitations at the acceptor sites, thereby hampering exciton diffusion and singlet–singlet annihilation while minimizing optical reabsorption loss.[27] This provides a means to reduce both linear and nonlinear internal losses in crystalline oligophenyl films. Optical losses could also be reduced by employing distributed- feedback structures superimposed onto the active material.[14,28] Printed grating structures on a suitable polymer coating on the *p*-6P film could serve as a cost-effective solution.

In conclusion, we studied laser action in epitaxially-grown oligophenyl nanofiber films under both femto- and nanosecond-pulsed excitation conditions at cryogenic and room temperature. Lasing threshold is almost independent of lattice temperature for femtosecond excitation, but is reduced by about two orders of magnitude when nanofibers are cooled from 300 to 80 K under slowly varying excitation conditions. This behavior primarily results from the dependence of exciton mobility on lattice temperature; as exciton mobility generally reduces with crystal cooling, the low-temperature improvement of lasing threshold is expected to be observable in other organic crystals. Inhibition of singlet bimolecular recombination at 80 K enables laser action in the monomolecular regime. Material doping and photonic engineering are proposed as effective strategies to overcome limitations imposed by nonlinear losses on lasing action at room temperature.

Experimental

The nanofiber films were grown by hot-wall epitaxy [7] on freshly cleaved (001)-oriented muscovite mica. Films with nanofibers ranging in height from ca. 100 to ca. 300 nm and in width from ca. 200 to ca. 350 nm were obtained for increasing growth times [21]. A continuous-flow, low-vibration cold-finger cryostat fed with liquid air was used to vary the sample temperature in the 80–300 K range. Ultrafast excitation experiments were performed using 150 fs long pulses delivered by an optical parametric amplifier (Light Conversion Topas) pumped by a Ti:sapphire amplified laser with 1 kHz repetition rate (Quantronix Integra, 1.5 mJ output energy). The optical emission was spectrally dispersed in a single spectrometer and temporally resolved with a visible streak camera having a temporal resolution of 20 ps. Nanosecond excitation experiments were carried out using 4 ns long pulses from an optical parametric oscillator pumped by a Q-switched neodymium-doped yttrium aluminum garnet (Nd:YAG) laser with 10 Hz repetition rate. The emission was sent through a single spectrometer and acquired by an image-intensified, time-gateable CCD camera with ca. 3 ns temporal resolution.

[1] I. D. W. Samuel, G. A. Turnbull, *Chem. Rev.* **2007**, *107*, 1272.

[2] T. Birendra-Singh, G. Hernandez-Sosa, H. Neugebauer, A. Andreev, H. Sitter, N. S. Sariciftci, *Phys. Status Solidi B* **2006**, *243*, 3329.

[3] a) J. Stampfl, S. Tasch, G. Leising, U. Scherf, *Synth. Met.* **1995**, *71*, 2125. b) A. Piaggi, G. Lanzani, G. Bongiovanni, A. Mura, W. Graupner, F. Meghdadi, G. Leising, M. Nisoli, *Phys. Rev. B* **1997**, *56*, 10133.

[4] a) M. Ichikawa, R. Hibino, M. Inoue, T. Haritani, S. Hotta, T. Koyama, Y. Taniguchi, *Adv. Mater.* **2003**, *15*, 213. b) R. Hibino, M. Nagawa, S. Hotta, M. Ichikawa, T. Koyama, Y. Taniguchi, *Adv. Mater.* **2002**, *14*, 119.

[5] F. Quochi, F. Cordella, R. Orrù, J. E. Communal, P. Verzeroli, A. Mura, G. Bongiovanni, A. Andreev, H. Sitter, N. S. Sariciftci, *Appl. Phys. Lett.* **2004**, *84*, 4454.

[6] H. Yanagi, T. Morikawa, *Appl. Phys. Lett.* **1999**, *75*, 187.

[7] A. Andreev, G. Matt, C. J. Brabec, H. Sitter, D. Badt, H. Seyringer, N. S. Sariciftci, *Adv. Mater.* **2000**, *12*, 629.

[8] F. Balzer, H.-G. Rubahn, *Appl. Phys. Lett.* **2001**, *79*, 3860.

[9] J. Kjelstrup-Hansen, H. H. Henrichsen, P. Bøggild, H.-G. Rubahn, *Thin Solid Films* **2006**, *515*, 827.

[10] F. Balzer, V. G. Bordo, A. C. Simonsen, H.-G. Rubahn, *Phys. Rev. B* **2003**, *67*, 115408.

[11] F. Quochi, F. Cordella, A. Mura, G. Bongiovanni, F. Balzer, H.-G. Rubahn, *Appl. Phys. Lett.* **2006**, *88*, 041106.

[12] F. Cordella, F. Quochi, M. Saba, A. Andreev, H. Sitter, N. S. Sariciftci, A. Mura, G. Bongiovanni, *Adv. Mater.* **2007**, *19*, 2252.

[13] M. Schiek, A. Lützen, R. Koch, K. Al-Shamery, F. Balzer, R. Frese, H.-G. Rubahn, *Appl. Phys. Lett.* **2005**, *86*, 153107.

[14] A. Rose, Z. Zhu, C. F. Madigan, T. M. Swager, V. Bulovic, *Nature* **2005**, *434*, 876.

[15] M. Pope, C. E. Swenberg, *Electronic Processes in Organic Crystals and Polymers*, Oxford University Press, New York **1999**.

[16] M. A. Baldo, R. J. Holmes, S. R. Forrest, *Phys. Rev. B* **2002**, *66*, 035321.

[17] P. A. Losio, Ch, Hunziger, P. Guenter, *Appl. Phys. Lett.* **2007**, *90*, 241103.

[18] G. Cerullo, G. Lanzani, S. De Silvestri, H.-J. Egelhaaf, L. Lüer, D. Oelkrug, *Phys. Rev. B* **2000**, *62*, 2429.

[19] T. Takenobu, S. Z. Bisri, T. Takahashi, M. Yahiro, C. Adachi, Y. Iwasa, *Phys. Rev. Lett.* **2008**, *100*, 066601.

[20] F. Quochi, F. Cordella, A. Mura, G. Bongiovanni, F. Balzer, H.-G. Rubahn, *J. Phys. Chem. B* **2005**, *109*, 21690.

[21] A. Andreev, F. Quochi, F. Cordella, A. Mura, G. Bongiovanni, H. Sitter, G. Hlawacek, C. Teichert, N. S. Sariciftci, *J. Appl. Phys.* **2006**, *99*, 034305.

[22] The recombination dynamics of singlet population density (N_S) is modeled by using the rate equation $dN_S/dt = -k_0 N_S - \kappa_{SS} N_S^2/2$, where k_0 is the monomolecular decay rate constant and κ_{SS} the singlet–singlet annihilation coefficient. Retrieval of the characteristic decay times is made after convolution of the calculated decay curve $N_S(t)$ with the detection response function $R(t)$, which is assumed a Gaussian shape with FWHM of 20 ps.

[23] A. Kadashchuk, A. Andreev, H. Sitter, N. S. Sariciftci, Y. Skryshevsky, Y. Piriatinski, I. Blonsky, D. Meissner, *Adv. Funct. Mater.* **2004**, *14*, 970.

[24] H. Wiesenhofer, E. Zojer, E. J. W. List, U. Scherf, J.-L. Brédas, D. Beljonne, *Adv. Mater.* **2006**, *18*, 310.

[25] Minor random variation in threshold femtosecond-pulsed fluence (typically a factor of two) observed across the 80–300 K temperature range at fixed sample positions suggests that linear absorption losses are negligible or weakly dependent on temperature. Temperature sensitivity of random optical feedback provided by recurrent fiber breaks may also explain an effect of lattice temperature on lasing threshold.

[26] C. Zenz, G. Cerullo, G. Lanzani, W. Graupner, F. Meghdadi, G. Leising, S. De Silvestri, *Phys. Rev. B* **1999**, *59*, 14336.

[27] M. Berggren, A. Dodabalapur, R. E. Slusher, Z. Bao, *Nature* **1997**, *389*, 466.

[28] T. Rabe, K. Gerlach, T. Riedl, H.-H. Johannes, W. Kowalsky, J. Niederhofer, W. Gries, J. Wang, T. Weimann, P. Hinze, F. Galbrecht, U. Scherf, *Appl. Phys. Lett.* **2006**, *89*, 081115.